

Hydrodynamic Doppler effect in flowing soap films

Kim Ildoo*

FG Research LLC, Bellevue, Washington 98004

(Dated: April 8, 2024)

Abstract

It is known for many years that the vorticity and the thickness fields in soap films are coupled and that the thickness wave propagates at the Marangoni wave speed. Based on the two observations, we propose a hypothesis that the vorticity field propagates at the Marangoni wave speed in flowing soap film channels. Using the hypothesis, we modify the point vortex model and find that the periodic array of vortices will have an expanded periodicity in the longitudinal direction, similar to the redshift of the Doppler effect. The theoretical prediction is compared with the experiments and we find that the hydrodynamic Doppler effect is present in soap film flows.

Experiments in physics take place in a model system. A model system is a simplified and approximated version of reality and is designed to capture the key physics under investigation. Ideally, the system is well understood and controlled to avoid unnecessary complication or undue uncertainties that may prevent us from a reproducible and consistent result.

This work concerns a soap film channel as a model system of a two-dimensional (2D) fluid. The soap film channel has been developed as a scientific instrument in late 1980s with seminal contributions by Couder *et al.* [1], Beizaie and Gharib [2], and Rutgers *et al.* [3], and since then it has been used to study 2D hydrodynamics. In specific, soap film channels are used to investigate cylinder wakes [4–7], the flow past elastic structures [8, 9], and 2D pipe flows [10, 11]. Most notably, a great advance has been made in our understanding of 2D decaying and forced turbulence [12, 13], including an important observation of the inverse cascade [14].

Despite numerous success stories, a soap film channel remains as one of capricious systems that requires a great caution to obtain consistent result. It is widely acknowledged by the community that the variation of flow speed alters the outcome of experiments a great deal, and many research groups persistently keep the flow speed constant. It is speculated that the variation of film thickness, accompanied with the variation of flow speed, creates the divergence in results. The apparent correlation between the flow speed and the film thickness is yet to be unpacked [15, 16], but even if we fully unpack the mystery, the question still remains: why and how does the variation of the film thickness affect the flow structure?

To answer this question, we bring to light two independent experiments. One finding in a flowing soap film is that the vorticity field and the thickness field are strongly correlated. Rivera *et al.* [17] directly measured the vorticity field using the particle image velocimetry and the thickness field using light scattering. They have shown that the two fields are coupled and suggest that the thickness and the vorticity behave as passive scalar, and therefore the correlation persists downstream [18]. Second finding is that the thickness field propagates at a certain speed called the Marangoni wave speed [19]. The stability of soap films is because of the elasticity E that arises from the presence of surfactants, and this dynamic process of stabilization naturally produces a 2D-compressible wave [20] travelling at the Marangoni wave speed $v_M = \sqrt{2E/\rho h}$ [1, 21, 22] where $E \approx 22 \text{ mN/m}$ in a typical setup of soap film channels [19].

Connecting the two findings, we hypothesize that the vorticity field is transmitted at the

speed v_M in a flowing soap film. In hydrodynamics, the characteristic velocity of the system is usually much slower than the propagation speed of the field because the high density of water renders both fast acoustic wave and high dynamic viscosity. In soap films, however, the 2D compressibility results in relatively slow propagation, normally at $v_M \sim 3$ m/s, compared to the typical flow speed of $u \sim 1.5$ m/s.

With the hypothesis in mind, we investigate whether the retardation effect creates a detectable change in the spatial arrangement of vortex street. In our theoretical investigation, we modify the point vortex model for finite propagation. In conventional framework, the flow is expressed as a gradient of a potential function ϕ and a stream function ψ , which together constitute an analytic function $W = \phi + i\psi$ in a complex plane. When the propagation is assumed to be instantaneous, the field is acquired by the integration using Green's function. In our modified framework, we assume the weak compressibility to keep the conventional definition of the complex potential [23], but we assume that the field is integrated over the source at the retarded time. It is inferred, as a corollary, that a vortex street is elongated in the longitudinal direction as $M \equiv u/v_M$ increases and produces an effect similar to the redshift of the Doppler effect.

The prediction of the theoretical model has confirmed by experiment. For vortex streets in soap films, we measure the ratio $q \equiv h/\ell$ between the transversal and longitudinal spacing h and ℓ between vortices and find that q decreases from 0.42 to 0.35 when M is varied from 0.1 to 0.8. The experimental observation strongly indicates that the retardation effect is substantial in flowing soap films and is consistent with the theoretical prediction.

The experiment is carried out in an inclined soap film channel, as discussed in literature [6, 24, 25]. Our channel is approximately 2 m long and inclined by 78° from the direction of the gravity. We use the soap solution made of 2% commercial dish-soap (P&G Dawn) and 98% of deionized water. The bulk kinematic viscosity is measured to be 0.0126 cm²/s.

The thickness and the mean flow speed of the soap film is varied by the flow rate of the soap solution. The continuity of the flow implies that the flow rate F of the soap solution is conserved throughout the channel [19, 26], i.e. $F = Wu\delta$, where W , u and δ are respectively the width, flow speed and thickness of the soap film. While we fix W at 3.6 cm, we vary F from 0.045 cm³/s to 0.64 cm³/s, and at the same time u is varied from 30 cm/s to 150 cm/s, measured by the particle tracking velocimetry. The mean thickness of the film is then derived from the relation $\delta = F/(Wu)$ and ranges from 3.5 μ m to 13 μ m. For a few

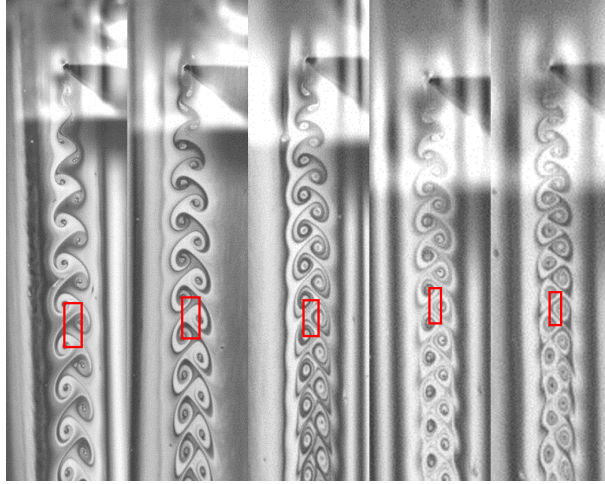


Figure 1. Vortex streets in the soap film at $Re \simeq 138$. (a) $u = 32$ cm/s and $D = 0.056$ cm, (b) $u = 38$ cm/s and $D = 0.047$ cm, (c) $u = 52$ cm/s and $D = 0.035$ cm, (d) $u = 64$ cm/s and $D = 0.027$ cm, and (e) $u = 77$ cm/s and $D = 0.024$ cm. The images are rescaled by D .

data points, we confirm that the estimate of δ agrees with the direct measurement using the transmittance of the polarized laser [27] within 10%.

The vortex streets are generated by inserting a circular cylinder into the soap film. The cylinder is made of titanium and is tapered up to the tip size $50 \mu\text{m}$. We vary the diameter D of the cylinder in the soap film from 0.0064 to 0.083 cm by changing the insertion depth which we precisely measure by a long-distance microscope. In this study, the Reynolds number, defined by $Re = UD/\nu$, ranges from 50 to 550 .

Next, the flow patterns are visualized by a fast video camera (Phantom V5, Vision Research) at 1900 fps. The flow channel is illuminated by the low-pressure sodium lamp (wavelength: 589 nm), and the interferogram is captured by the video recording. As discussed earlier, the thickness variation is correlated with the vorticity variation [17], and therefore the interferogram provides us a direct means to measure flow structures without any post-processing of images.

Figure 1 shows the flow structure captured at various u and D . From (a) to (e), $u = 32, 38, 52, 64$ and 77 cm/s, and $D = 0.056, 0.047, 0.035, 0.027$ and 0.024 cm, respectively. Even though u and D are varied, Re is controlled to be almost invariant at $138(\pm 4)$. The red rectangles highlight the longitudinal and transversal spacing between vortices, ℓ and h , respectively.

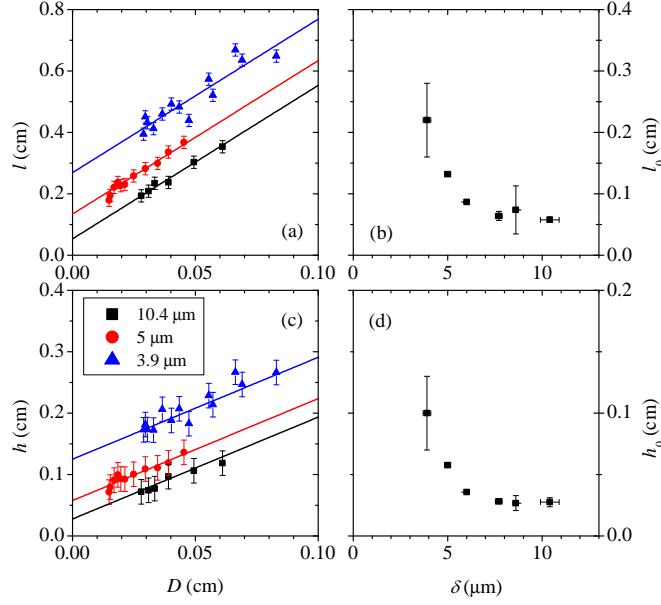


Figure 2. The measurement of ℓ and h . (a) The longitudinal spacing ℓ is linearly proportional to D with (b) the intercept that depends on u . (c,d) A linearity is also observed for h .

In Fig. 2, we show the measurements of the ℓ and h with respect to D . We find that both ℓ and h are linearly proportional to D as demonstrated in Refs. [5, 6] after the data are grouped by their respective film thickness as presented in Fig. 2(a,c). The scaling relation follows the linear form $\ell = \ell_0(\delta) + \alpha D$ and $h = h_0(\delta) + \beta D$, where α and β are the proportionality constants and ℓ_0 and h_0 are the intercepts. The intercepts, both ℓ_0 and h_0 , are decreasing functions of δ , as depicted in Fig. 2(b,d). For a soap film of $\delta \simeq 3 \mu\text{m}$ and $u \simeq 34 \text{ cm/s}$, the intercepts can be as high as $\ell_0 = 0.27 \text{ cm}$ and $h_0 = 0.13 \text{ cm}$. We also calculate the values of the slopes: $\alpha = 5.00 \pm 0.15$ and $\beta = 1.66 \pm 0.12$. Using the above information, we infer that the ratio $q \equiv h/\ell$ can be as high as $0.48 (\approx h_0/\ell_0)$ for small δ and D , and that as small as $0.33 (\approx \beta/\alpha)$ in the other extreme. We remark that this range of q is greater than the prediction of the original point vortex model [28–30], which implies that only vortex streets with $q \simeq 0.28$ are stable.

Finally, we obtain q from the individual measurement of ℓ and h . The calculated q is plotted in Fig. 3 with respect to a dimensionless number $M = u/v_M \propto \sqrt{\delta}u$, that is analogous to Mach number in aerodynamics. The data clearly indicate that the spatial arrangement of vortex streets, quantified by q , is affected by either u or δ , and that the change is characterized by the expansion of the periodic structure in the longitudinal direction.

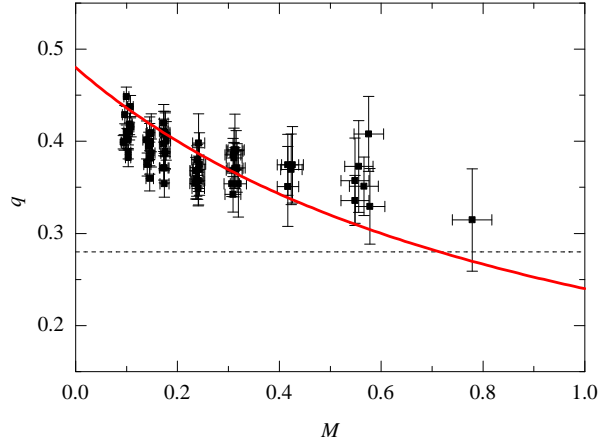


Figure 3. The measurement of q with respect to $M = u/v_M$. The solid curve shows the calculation of Eq. (5) using $q_0 = 0.48$, and the dotted line shows $q = 0.28$ of the original point vortex model.

To reveal the physical origin of the change, we develop a modified point vortex model which explores a hypothesis that the vorticity field propagates at the Marangoni wave speed v_M . This hypothesis is based on the experimentally observed facts: i) in soap films, it is well understood that the vorticity field is strongly correlated with the thickness field [17], and ii) it is known that the thickness field propagates at the Marangoni wave speed, which depends on the mean thickness δ and the elasticity E , that is, $v_M = \sqrt{2E/\rho\delta}$ [19].

Throughout the current theoretical analysis we assume that the soap film is compressible, yet the compressibility is weak enough so that we can still use the point vortex model with a minimum modification. For such a flow, the stream function $\psi(z)$ of the flow satisfies the inhomogeneous Laplace equation

$$\nabla^2\psi = \omega(z), \quad (1)$$

where $\omega(z)$ is the vortex density function. In the conventional point vortex model, Eq. (1) is solved by using Green's function, which in 2D is $G(z, z') = (2\pi)^{-1} \log |z - z'|$, and it follows that $\psi(z) = \int G(z, z')\omega(z')dz'$. In the modified point vortex model, the integration is evaluated at the retarded time $t_r = t - |z - z'|/v_M$ as

$$\psi(z, t) = \int G(z, z')\omega(z', t_r)dz'. \quad (2)$$

For a vortex street drifting at u along the real axis, $\omega(z, t) = \kappa \sum_n \delta(z - ut - nl) - \sum \kappa \delta(z - ut - nl - l - ih)$, where κ is the circulation of each vortex.

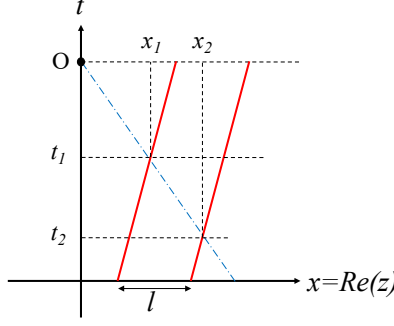


Figure 4. The diagram shows the retardation effect of the field propagation produces an effective elongation of a vortex street. The time flows along the ordinate, and a pair of vortices, whose trajectories are shown by solid lines, moving away from the origin. When transmitted by the Marangoni wave (the dash-dot line), the information of the location x_1 and x_2 of the vortices is carried out to the origin.

Equation (2) is not easily integrated because t_r is not fixed. We invoke the procedure to solve the Liénard-Wiechert potential in relativistic electromagnetic theory [31, 32]. First we choose a time t_1 , which is the retarded time for some point in the interior of the vortex distribution. Next, we change the integration over z' to an integration over z_1 . Then, Eq. (2) becomes

$$\psi(z, t_r) = \frac{1}{2\pi} \frac{\log R}{1 + \vec{v}' \cdot \hat{n}'/v_M} \int \omega(z_1, t_1) dz_1, \quad (3)$$

where $R\hat{n}' = z' - z$ and \vec{v}' the velocity of the vortex distribution at t_1 . The integration of Eq. (3) for a pair of vortex arrays is intractable, so, instead, we solve for a simpler case where a single vortex is moving at u along the real axis, i.e. $\omega(z, t) = \kappa\delta(z - ut)$. Then we get

$$\psi(z, t) = \frac{\kappa}{2\pi} \frac{\log R}{1 + M}. \quad (4)$$

To geometrically interpret Eq. (4), we use a diagram analogous to the light cone of relativity. Figure 4 depicts two vortices separated by ℓ traveling at the speed u (a pair of thick solid lines). When the wave speed is v_M , the flow field at the origin (O) is determined by the location x_1 and x_2 of the vortices at the retarded time t_1 and t_2 . The geometric analysis suggests that $t_1 - t_2 = (x_2 - x_1)/v_M = (\ell - x_2 + x_1)/U$, implying $(x_2 - x_1) = \ell\gamma$, where $\gamma = (1 + M)^{-1}$. At the origin, the spatial arrangement of vortices is determined to satisfy $q_0 = h/(x_2 - x_1)$, where q_0 is the value of q when $M = 0$. Therefore, q is, in the lab

frame,

$$q = h/\ell = \gamma q_0. \quad (5)$$

Physical interpretation regards this phenomenon similar to the redshift of the Doppler effect because it occurs only when the vortices recede from the origin.

We have compared the theoretical prediction of the modified point vortex model with experimental measurements. In Fig. 3, we evaluate Eq. (5) using $E = 22$ mN/m [19] and $q_0 = 0.48$, and the calculation is plotted with the solid line. We find that the theoretical curve matches with data within the margin of error, and this overall trend shows that the retardation effect may be substantial in a soap film flow.

Before closing the discussion, we also review the possibility that the variation of q is solely due to the change of the viscosity of the film which in effect is due to the change in its thickness. In literature, the viscosity of a soap film is described by the Trapeznikov relation $\eta = 2\eta_s + \eta_b\delta$, where η_b is the dynamic viscosity of the bulk liquid and η_s is the contribution of the surface viscosity [33]. The relation indicates that the dynamic viscosity is higher for thicker films. Contrary to literature [34] which states that the increasing viscosity acts to increase q , our thicker film yields to lower q . Also, when the Trapeznikov relation is divided by the 2D density $\rho_2 = \rho_3\delta$, it becomes the kinematic viscosity relation $\nu = 2\nu_s + \nu_b$, which does not depend on thickness. This concludes that the effect of the viscosity is not present, or even if it does, not significant.

To summarize, we have proposed a hypothesis that the vorticity field propagates at the Marangoni wave speed in flowing soap films. This hypothesis is based on two experiments: one is that the vorticity field is coupled with the thickness field, and the other is that the thickness variation propagates at the Marangoni wave speed. Based on the hypothesis, we propose the retarded point vortex model to describe the morphological change of the vortex arrangement in flowing soap films. The model predicts that the longitudinal periodicity of the vortex shedding increases by a factor of $(1 + u/v_M)^{-1}$, as the flow speed u of the soap film flow approaches the wave speed v_M . The model is compared with the experimental data using the cylinder wake, and we find that they agree within the margin of error.

The study suggests that the retardation effect of the field may present in soap film flows. If we regard the caveats of the study as true statements, the discussed hypothesis is indeed true. This new finding is potentially useful for improving measurement techniques in fluid experiments. If the current conclusion is determined to be false, then either postulate is

false. I speculate that in such case the general belief that the vorticity field is captured by the interferogram is in peril and needs reconsideration.

In any case, the soap film channel should be considered as two-dimensional Navier-Stokes system only under a specific context.

* ildoo.kim.phys@gmail.com

- [1] Y. Couder, J. M. Chomaz, and M. Rabaud, On the hydrodynamic of soap films, [Physica D **37**, 384 \(1989\)](#).
- [2] M. Beizaie and M. Gharib, Fundamentals of a liquid (soap) film tunnel, [Exp. Fluids **23**, 130 \(1997\)](#).
- [3] M. A. Rutgers, X.-L. Wu, and W. B. Daniel, Conducting fluid dynamics experiments with vertically falling soap films, [Rev. Sci. Instrum. **72**, 3025 \(2001\)](#).
- [4] P. Vorobieff and R. E. Ecke, Cylinder wakes in flowing soap films, [Phys. Rev. E **60**, 2953 \(1999\)](#).
- [5] P. Roushan and X. L. Wu, Structure-Based Interpretation of the Strouhal-Reynolds Number Relationship, [Phys. Rev. Lett. **94**, 054504 \(2005\)](#).
- [6] I. Kim and X. L. Wu, Unified Strouhal-Reynolds number relationship for laminar vortex streets generated by different-shaped obstacles, [Phys. Rev. E **92**, 043011 \(2015\)](#).
- [7] I. Kim, Separated rows structure of vortex streets behind triangular objects, [J. Fluid Mech. **862**, 216 \(2019\)](#).
- [8] S. Jung, K. Mareck, M. J. Shelley, and J. Zhang, Dynamics of a Deformable Body in a Fast Flowing Soap Film, [Phys. Rev. Lett. **97**, 134502 \(2006\)](#).
- [9] L. Ristroph and J. Zhang, Anomalous Hydrodynamic Drafting of Interacting Flapping Flags, [Phys. Rev. Lett. **101**, 194502 \(2008\)](#).
- [10] T. Tran, P. Chakraborty, N. Guttenberg, A. Prescott, H. Kellay, W. I. Goldburg, N. Goldenfeld, and G. Gioia, Macroscopic effects of the spectral structure in turbulent flows, [Nat. Phys. **6**, 438 \(2010\)](#).
- [11] R. T. Cerbus, C.-C. Liu, G. Gioia, and P. Chakraborty, Laws of Resistance in Transitional Pipe Flows, [Phys. Rev. Lett. **120**, 054502 \(2018\)](#).
- [12] H. Kellay, X.-L. Wu, and W. I. Goldburg, Experiments with Turbulent Soap Films, [Phys.](#)

- [Rev. Lett. **74**, 3975 \(1995\).](#)
- [13] B. K. Martin, X.-L. Wu, W. I. Goldburg, and M. A. Rutgers, Spectra of Decaying Turbulence in a Soap Film, [Phys. Rev. Lett. **80**, 3964 \(1998\).](#)
 - [14] M. A. Rutgers, Forced 2D Turbulence: Experimental Evidence of Simultaneous Inverse Energy and Forward Enstrophy Cascades, [Phys. Rev. Lett. **81**, 2244 \(1998\).](#)
 - [15] M. A. Rutgers, X.-L. Wu, R. Bhagavatula, A. A. Petersen, and W. I. Goldburg, Two-dimensional velocity profiles and laminar boundary layers in flowing soap films, [Phys. Fluids **8**, 2847 \(1996\).](#)
 - [16] A. Sane, S. Mandre, and I. Kim, Surface tension of flowing soap films, [J. Fluid Mech. **841**, R2 \(2018\).](#)
 - [17] M. Rivera, P. Vorobieff, and R. E. Ecke, Turbulence in flowing soap films: Velocity, vorticity, and thickness fields, [Phys. Rev. Lett. **81**, 1417 \(1998\).](#)
 - [18] P. Vorobieff, M. Rivera, and R. E. Ecke, Soap film flows: Statistics of two-dimensional turbulence, [Phys. Fluids **11**, 2167 \(1999\).](#)
 - [19] I. Kim and S. Mandre, Marangoni elasticity of flowing soap films, [Phys. Rev. Fluids **2**, 082001\(R\) \(2017\).](#)
 - [20] G. I. Taylor, The Dynamics of Thin Sheets of Fluid. II. Waves on Fluid Sheets, [Proc. Roy. Soc. London A **253**, 296 \(1959\).](#)
 - [21] J. Lucassen, M. Van den Tempel, A. Vrij, and F. Hesselink, Waves in thin liquid films, [Proc. K. Ned. Akad. Wet. B **73**, 109 \(1970\).](#)
 - [22] A. Vrij, F. Hesselink, J. Lucassen, and M. Van den Tempel, Waves in thin liquid films, [Proc. K. Ned. Akad. Wet. B **73**, 124 \(1970\).](#)
 - [23] D. G. Crowdy and V. S. Krishnamurthy, Speed of a von kármán vortex street in a weakly compressible fluid, [Phys. Rev. Fluids **2**, 114701 \(2017\).](#)
 - [24] X.-L. Wu, R. Levine, M. A. Rutgers, H. Kellay, and W. I. Goldburg, Infrared technique for measuring thickness of a flowing soap film, [Rev. Sci. Instrum. **72**, 2467 \(2001\).](#)
 - [25] D. Georgiev and P. Vorobieff, The slowest soap-film tunnel in the Southwest, [Rev. Sci. Instrum. **73**, 1177 \(2002\).](#)
 - [26] T. Tran, P. Chakraborty, G. Gioia, S. F. Steers, and W. I. Goldburg, Marangoni Shocks in Unobstructed Soap-Film Flows, [Phys. Rev. Lett. **103**, 104501 \(2009\).](#)
 - [27] I. Kim and X. L. Wu, Tunneling of micron-sized droplets through soap films, [Phys. Rev. E](#)

- [82](#), 026313 (2010).
- [28] T. von Kármán, Über den Mechanismus des Widerstandes, den ein bewegter Körper in einer Flüssigkeit erfährt, Gott. Nachr. Math.-Phys. Klasse , 509 (1911).
 - [29] T. von Karman and A. Henze, On the mechanism of the drag a moving body experiences in a fluid, [Prog. Aerosp. Sci. 59](#), 13 (2013).
 - [30] P. G. Saffman, *Vortex Dynamics* (Cambridge, 1992).
 - [31] J. D. Jackson, *Classical Electrodynamics 3/e* (Wiley, 1998).
 - [32] J. R. Reitz, F. J. Milford, and R. W. Christy, *Foundation of electromagnetic theory 4/e* (Addison-Wesley, 1992).
 - [33] V. Prasad and E. R. Weeks, Flow fields in soap films: Relating viscosity and film thickness, [Phys. Rev. E 80](#), 026309 (2009).
 - [34] S. G. Hooker, On the Action of Viscosity in Increasing the Spacing Ratio of a Vortex Street, [Proc. Roy. Soc. London A 154](#), 67 (1936).